



ELSEVIER

1 January 2002

Optics Communications 201 (2002) 165–171

OPTICS  
COMMUNICATIONS

www.elsevier.com/locate/optcom

# LD pumped intracavity frequency-doubled and frequency-stabilized Nd:YAP/KTP laser with 1.1 W output at 540 nm

Xiaoying Li, Qing Pan, Jietai Jing, Changde Xie, Kunchi Peng\*

*State Key Laboratory of Quantum Optics and Quantum Optic Devices, Institute of Opto-Electronics, Shanxi University, Taiyuan, Shanxi, 030006, PR China*

Received 16 May 2001; received in revised form 26 October 2001; accepted 31 October 2001

## Abstract

A compact LD pumped intracavity frequency-doubled and frequency-stabilized ring Nd:YAP/KTP laser with high output up to 1.1 W at 540 nm is achieved. In the design of the laser configuration, the anisotropic characteristics of Nd:YAP optical biaxial crystal are taken into account. A quarter-wave plate is placed between the Faraday rotator and the  $\alpha$ -cut KTP to ensure the output fundamental wave from KTP in pure linear-polarization paralleling to that of the oscillating laser and unidirectional operation of laser. Due to rigorously temperature controlling on KTP crystals and optimizing design of resonator, the stable single-frequency green output is obtained. The intensity fluctuation is less than  $\pm 1.5\%$ , and frequency stability is better than  $\pm 550$  kHz by means of a standard frequency locking technology with F-P cavity. © 2002 Published by Elsevier Science B.V.

## 1. Introduction

The intracavity frequency-doubled and frequency-stabilized Nd:YAP laser is an important light source for non-linear and quantum optics. Since the wavelength of 1080 nm emitted by Nd:YAP is able to realize type II non-critical phase-matching in an  $\alpha$ -cut KTP crystal [1], the effect of beam walk-off is eliminated and the parameter conversion efficiency is increased relative to that with the angular phase-matching crystal [2].

The arc-lamp pumped Nd:YAP/KTP laser has been used successfully to produce EPR beams with high quantum correlation [3,4]. The laser has potentially important application in the research field of quantum information. The quantum entangled beams employed for practical quantum information processing [5,6], such as quantum teleportation and quantum dense coding etc. should have long-term stability and high quantum correlation, so a laser source with long-term frequency stability, low intensity fluctuation and high output power is required. However, the lamp-pumped laser system is difficult to satisfy these requirements. Though commercial systems giving multi-watt output with single-frequency have been available for some

\* Corresponding author.

E-mail address: kcpeng@sxu.edu.cn (K. Peng).

time, there is no one with suitable wavelength to realized type II non-critical phase-matching in KTP crystal. Therefore we designed and accomplished a fiber-coupled diode array end-pumped intracavity frequency-doubled continuous Nd:YAP/KTP laser. The bow-tie resonator configuration with four mirrors is more compact than that of the previous lamp-pumped one with six mirrors [7].

For all-solid-state laser pumped by high power LD, the thermal effect of gain medium affecting the laser performance seriously has attached more interest for a long time. The temperature distribution in the laser crystal end-pumped by LD is quite different from that pumped by lamp. For the lamp-pumped laser, one usually considers that the laser crystal is uniformly pumped in axial direction, so temperature distribution in laser crystal is different only in cross-section. While in a LD end-pumped laser, in order to realize the mode match between the pumping beam and oscillating laser, the pumping beam is collimated into the crystal with a very small size. The power density of pump light and the temperature distribution resulting from pump heating is not uniform in three dimensions. The complexity of temperature distribution in end-pumped laser is further increased due to edge-cooling. Although end-pumping is an efficient way for all-solid-state laser, scaling end-pumping to high power is not easy [8,9]. At the power well below the fracture limit, the thermal distortion and strain-induced birefringence can significantly degrade laser performance. For the anisotropic crystal Nd:YAP, thermally induced birefringence is not a problem, but thermal distortion leads to both thermal focusing and spherical aberration. The cavity should be designed to satisfy the condition that the mode size in laser crystal is smaller than pump size to reduce the influence of spherical aberration to a certain extent.

The difficulties with the intracavity-doubled laser are due to the presence of green problem. Much research work has been done to overcome the greater intrinsic complexity of the intracavity-doubled devices [10–12]. The usual methods are eliminating spatial hole burning, controlling the polarization in doubling crystal and control the temperature of the doubling crystal to make it a

full-wave plate. Since in the process of type II non-critical phase-matching, the doubling efficiency closely depends on the temperature, it is difficult to control the temperature of KTP to make the KTP crystal playing a role of a full-wave plate and to maintain high doubling efficiency at the same time just by tuning the temperature of the crystal.

In our design, utilizing the anisotropic characteristic of Nd:YAP crystal and inserting a quarter-wave plate between the Faraday rotator and KTP crystal, the polarization orientation in laser crystal and frequency-doubling crystal and unidirectional operation of laser are ensured without extra inserted polarizer. The laser with a frequency-locking system can operate stably for several hours. Up to 1.1 W green output at 540 nm with the frequency-stability of  $\pm 550$  kHz is achieved, and its intensity fluctuation is less than  $\pm 1.5\%$ .

## 2. Experiment arrangement

The experiment setup is shown in Fig. 1. The main features are a Nd:YAP laser rod pumped by a fiber-coupled diode array whose beam size is confined by a focusing system, a four mirror cavity geometry employed to permit tight focusing the fundamental wave into the KTP doubling crystal, a Faraday rotator combined with a half-wave plate and a quarter-wave plate at 1080 nm to enforce unidirectional operation (see Section 3 for details).

Our experiment was carried out using a laser rod Nd:YAP, with Nd concentration of 1.0%, with 3 mm in diameter and 5 mm in length (purchase from Scientific Material, USA). It is cut along *b*-axis, flat/flat end, coated one side with AR 1080 nm/803 nm and another side with AR 1080 nm. The YAP host material ( $\text{YAlO}_3$ ) is biaxial crystal, and therefore the neodymium absorption and emission spectra are polarization dependent. For the Nd:YAP with Nd concentration of 1.0%, there are two absorption peak near 801 and 807 nm for *E//a* and three absorption peaks near 803, 805 and 807 nm for *E//c*. The strongest absorption peak is for *E//c* at 803 nm [13]. The highest gain emission at 1080 nm is polarized parallel to the *c*-axis [13]. In order to adjust conveniently, we put the *c*-axis

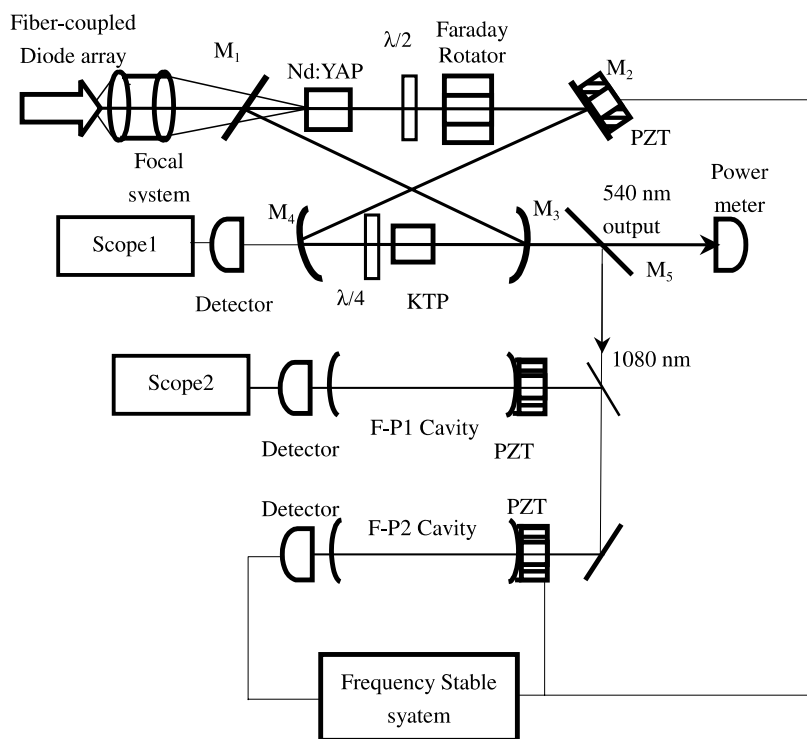


Fig. 1. Experimental setup of intracavity doubling fiber-coupled diode array end-pumped Nd:YAP/KTP laser.

of the Nd:YAP laser rod parallel to the s-polarization of the cavity mirrors (vertically).

The pumping source used in our experiment is a commercially available fiber-coupled diode array (FAP-808-16c-800-B, produced by Coherent), with maximum output power of 16 W in a circular-polarization. The peak emission wavelength was temperature tuned to the absorption peak of Nd:YAP crystal at 803 nm. The coupling fiber has core diameter of 800  $\mu\text{m}$  with a N.A. of 0.2. The output of the fiber was focused by a focusing system, which consists of two lenses with focal length of 30 mm and has a coupling efficiency of 90% at 803 nm. Pump spot size imaged on the laser rod is approximately 480  $\mu\text{m}$  diameter.

Total length of the four-mirror cavity is approximately 500 mm. Mirror  $M_4$  is mounted on a translator to change the distance between  $M_3$  and  $M_4$  to adjust the mode size in Nd:YAP crystal. The cavity mirror parameters are as follows: input coupling mirror  $M_1$  is a plane mirror with a high reflection (>99.7%) at 1080 nm and high trans-

mission ( $\sim 96\%$ ) at 803 nm,  $M_2$  is a plane mirror with a high reflection (>99.9%) at 1080 nm,  $M_3$  is a concave mirror with 100 mm radius of curvature and coated with high reflection (>99.98%) at 1080 nm, output coupling mirror  $M_4$  is also a concave mirror with 100 mm radius of curvature coated with high reflection (>99.6%) at 1080 nm and antireflection ( $\sim 96\%$ ) at 540 nm. The 10 mm long  $\alpha$ -cut KTP crystal with the section of  $3 \times 3 \text{ mm}^2$  coated with antireflection at both 1080 and 540 nm to minimize insertion losses is aligned with  $b$ - and  $c$ -axis at  $45^\circ$  with respect to the  $c$ -axis of Nd:YAP crystal and placed to the position of the beam waist of the oscillating laser between  $M_3$  and  $M_4$ . The KTP crystal is placed in a copper oven, which is temperature-controlled by a thermoelectric oven to get the highest doubling efficiency. The Faraday medium is a 3 mm  $\times$  5 mm TGG crystal (both end facets are antireflectively coated at 1080 nm), producing a polarization rotation of  $6^\circ$  at 1080 nm. A Faraday rotator, a quarter-wave plate and a half-wave plate at 1080 nm confirms the correct

polarization and unidirectional operation of laser.  $M_5$  is a dichroic mirror coated with high reflection at 1080 nm and antireflection at 540 nm. The reflected 1080 nm laser from  $M_5$  was introduced into F-P1 and F-P2 cavity, which are two reference cavities with a Invar structure, with a free spectrum of 1500 MHz, and a finenesses of 150 and 410, respectively. The laser mode was monitored by scanning the F-P1 cavity. The F-P2 cavity was combined with a frequency stability system to lock the laser frequency.

In order to removing the heat instantaneously from the gain medium to maintain the efficient operation of laser, the Nd:YAP crystal is wrapped with In foil and put into a copper sink, which is mounted on a thermoelectric cooler. In this way a stable temperature distribution in the laser crystal was achieved under a certain pump level.

### 3. Design principle

One key point of this resonator design at high pump power is that the  $TEM_{00}$  mode size in the laser crystal should be smaller than the pump beam size. This behavior is in contrast to the situation at low pump power, at which it is generally accepted that the laser mode size should be at least as large as the pump beam size to ensure both  $TEM_{00}$  operation and a high slope efficiency. Because at high powers the aberrations accompanying the strong thermal lens in the laser rod produce greater losses in the wings of the inversion distribution, therefore a smaller  $TEM_{00}$  laser mode size is favorable [9]. Obviously, the  $TEM_{00}$  mode size should not be too small, otherwise high-order transverse mode would also be excited.

Because thermal effects of laser crystal affect the laser performance seriously, we measured the focal length  $F_t$  of Nd:YAP crystal at first, the function curve of the focal length verses pump power was shown in Fig. 2. At the pump power 10 W, the focal length of the edge cooled laser rod is about 150 mm.

The design of resonator confirms the condition of stable mode operation  $|A + D| \leq 2$ , where  $A$  and  $D$  are elements of the ABCD transmission matrix of the laser cavity. In the numerical calculation,

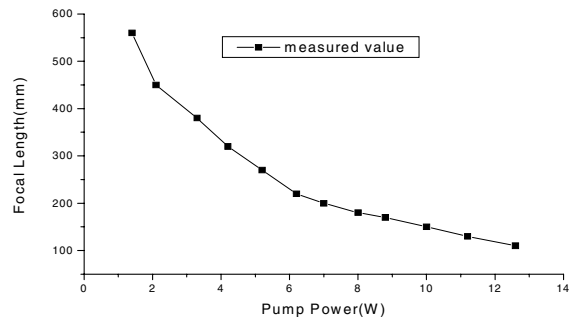


Fig. 2. Thermal focal length of  $\varnothing 3 \text{ mm} \times 5 \text{ mm}$  Nd:YAP crystal varies via pump power.

the front facet of Nd:YAP is chosen as the reference plane, the distances between which to  $M_3$  and  $M_4$  are  $L_2 = 165 \text{ mm}$  and  $L_3 = 205 \text{ mm}$ , respectively. Fig. 3 is the diagram of the distance  $L_1$  between  $M_3$  and  $M_4$  versus the thermal focal length ( $F_t$ ) of laser rod, the shadow region is the stable region, in which the laser can stably operate. For our system with the focal length of 150 mm, a large range of  $L_1/2$  from 40 to 69 mm is in the stable operation region. Fig. 4 shows that the mode size  $\omega_p$  in Nd:YAP varies via  $L_1$ , when  $L_1/2$  is changed from 50 to 65 mm, the  $\omega_p$  varies from 0.16 to 0.35 mm continuously. Thus we can conveniently match the pump mode with the cavity mode to get higher output. In our experiment, when  $L_1$  is taken about 125 mm (the radius of beam waist between  $M_3$  and  $M_4$  is about  $50 \mu\text{m}$ ), the fundamental wave

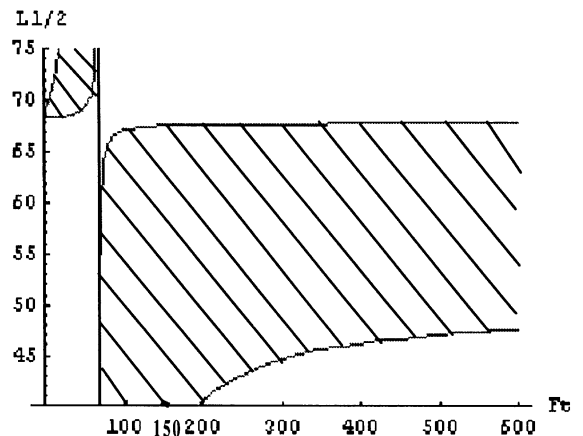


Fig. 3. Sketch map of the cavity stable region.

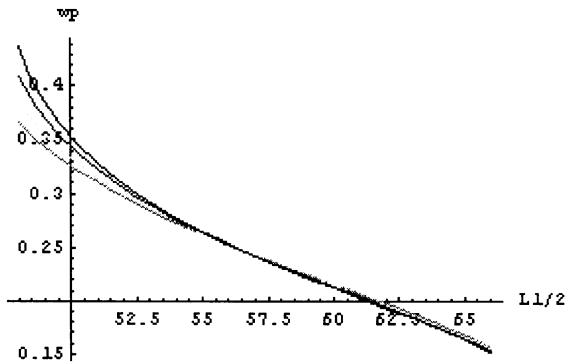


Fig. 4. Mode size of laser in Nd:YAP rod versus the distance  $L_1/2$ .

output reaches to the maximum without intracavity frequency doubler. While the frequency doubler, an  $\alpha$ -KTP crystal with 10 mm length, is inserted into the cavity, the efficient length of  $L_1$  is changed, so  $L_1$  is extend to about 129 mm to obtain the highest second harmonic output [7].

It is well known that intracavity frequency-doubled laser with single-frequency and stable output requires unidirectional operation to eliminate the spatial hole burning and the polarization of incident beam on the KTP should be at  $45^\circ$  with respect to the  $b$ - and  $c$ -axis of the crystal to ensure the balance of  $e_1$  and  $e_2$  polarization components [10,14]. Due to the dispersion, the indices of refraction  $n_{e_1}$  and  $n_{e_2}$  of the polarized components  $e_1$  and  $e_2$  along the  $b$  and  $c$  axes are different and the extra phase-difference  $\delta = (2\pi(n_{e_1} - n_{e_2})l_c)/\lambda$  ( $l_c$  is the length of KTP crystal,  $\lambda$  is the fundamental laser wave length) is added between  $e_1$  and  $e_2$  after a single-passing. The value of  $\delta$  depends upon the temperature of the KTP because of the temperature-dependence of the refractivities [14]. For the type II angular phase-matching KTP crystal, usually the dispersion can be compensated by tuning the temperature of crystal to make  $\delta = m2\pi$  ( $m$  is integer) [11,12]. But in the case of the type II non-critical phase-matching this method is unfitted. For the KTP crystal used in our experiment, its doubling efficiency versus temperature is presented in Fig. 5, there is homonic output within a wide range from 40 to 70  $^\circ\text{C}$ , and it is sensitive to temperature, we also can see, at the temperature

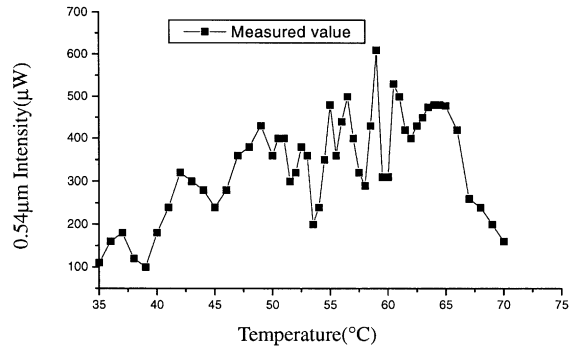


Fig. 5. 0.54  $\mu\text{m}$  output versus temperature, when a-cut KTP is single passed by 400 mW 1.08 mm laser with the polarization at  $45^\circ$  relative to  $b$ - and  $c$ -axis of KTP.

range 63–66  $^\circ\text{C}$ , the KTP crystal has higher doubling efficiency which is less sensitive to temperature, so it is a suitable temperature to obtain higher conversion efficiency and stable output. Fig. 6 is the measured curve of phase-difference  $\delta$  versus the temperature of the  $\alpha$ -cut KTP crystal, which shows the birefringence effect of the KTP. It is obvious, the phase-difference of  $2\pi$  corresponds to a temperature tuning range over 28  $^\circ\text{C}$  (see Fig. 6), which is far from the temperature (63–66  $^\circ\text{C}$ ) for the efficient and stable frequency-doubling. When the temperature of crystal is tuned to the optimal phase-matching point, the extra phase-difference  $\delta$  generally is not the integer factor of  $2\pi$ . It is easy to be demonstrated through a simple calculation that if a quarter-wave plate is placed behind the KTP crystal with  $45^\circ$  included angle between their principle axes, the combination of

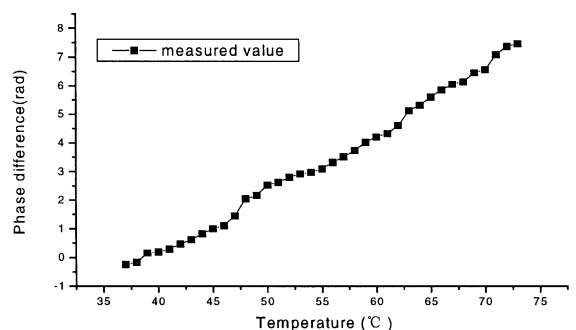


Fig. 6. The dependence of phase-difference on the temperature of KTP crystal.

the two birefringent elements KTP and  $\lambda/4$  wave plate plays a role of a polarization rotator for a incident light linear-polarized at  $45^\circ$  relative to  $e_1$  and  $e_2$  polarization in KTP. The polarization of output light from the KTP will rotate a angle  $\gamma = \delta/2$ . In this case, the KTP crystal,  $\lambda/4$  wave plate and Faraday rotator and  $\lambda/2$  wave plate (see Fig. 1) compose also a polarization rotator, which makes the polarization of laser transmitting from the Nd:YAP rotating an angle  $\Phi = 2\theta - a_0 + \delta/2$  after a round-trip in the resonator, where  $\theta$  is the included angle between the principal axis of  $\lambda/2$  wave plate and the  $c$ -axis of Nd:YAP laser crystal,  $a_0$  is the angle rotated by TGG in a single-passing. For the certain  $a_0$  and  $\delta$ , we can rotate the  $\lambda/2$  wave plate to adjust the angle  $\theta$  making  $\Phi = 2m\pi$  ( $m$  is an integer), so that the polarization of oscillating laser in the Nd:YAP is always parallel to its  $c$ -axis to satisfy the requirement of high efficient emitting. At the same time the balance of  $e_1$  and  $e_2$  polarization in the KTP crystal is also confirmed due to the  $45^\circ$  include angle between the  $c$ -axis of Nd:YAP and the principal axis of KTP.

#### 4. Experiment results

When the laser is pumped above the threshold of 1.4 W, and the temperature of KTP is tuned to the optimal phase-matching point ( $64.3^\circ\text{C}$ ) for SHG, green light at 540 nm is produced. The function of the output power versus incident pump power is shown in Fig. 7. The green output up to 1.1 W is obtained while the incident pump power is 10 W. When the pump power increased further

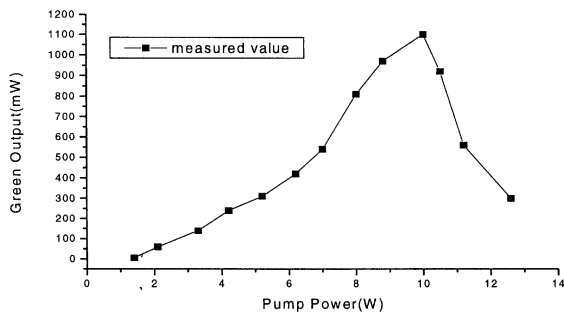


Fig. 7. Green output power versus pump power.

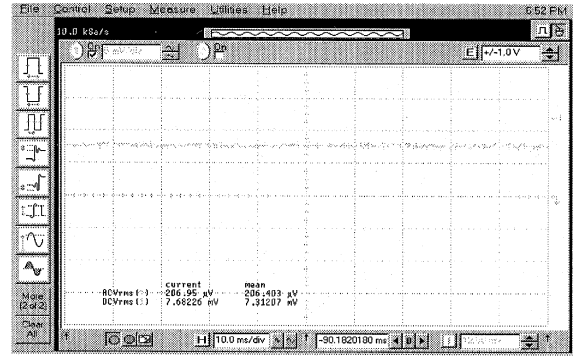


Fig. 8. Fluctuation of green output.

more, the green output started to decline, eventually disappeared, due to the increased aberration accompanying the high pump power and the shortened thermal focal length which move the configuration of laser cavity out of the stable range. Fig. 8 shows the output power fluctuation of green laser at 540 nm at the average power of 1.1 W and the fluctuation is less than  $\pm 1.5\%$ . The transmission curve of the fundamental wave through a scanned reference cavity F-P1 (Fig. 9) demonstrates that the laser operates in a single-longitudinal mode. Fig. 10 plots the frequency drift of fundamental wave with the frequency-locking system on. The frequency stability of the second harmonic light given in Fig. 10 is better than  $\pm 550$  kHz.

When the green output is 1.1 W, the fundamental leakage through  $M_4$  is about 120 mW, corresponds to a circulating power of about 30 W.

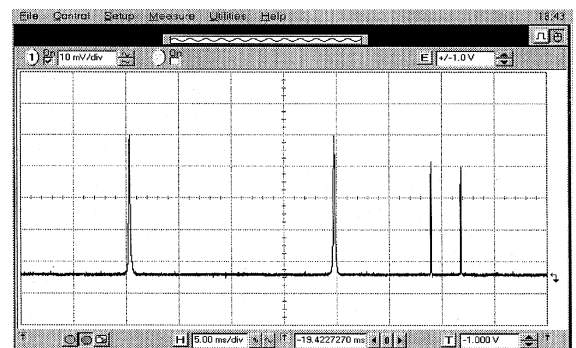


Fig. 9. Fundamental wave transmission through the scanning F-P1 cavity.

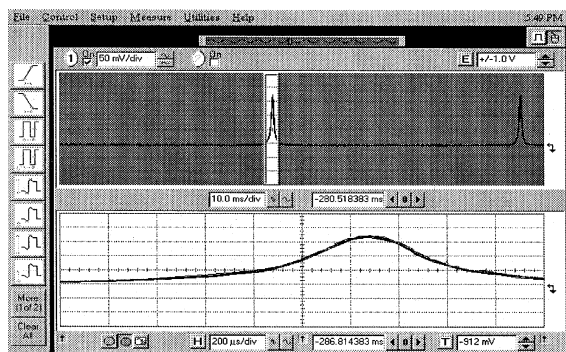


Fig. 10. Frequency stability of the fundamental wave through the scanning F-P1 cavity.

The result of effective non-linearity (the ratio of the harmonic output to the square of circulating fundamental power) is approximately  $1.27 \times 10^{-3} \text{ W}^{-1}$ , which agree with theoretical result [15]  $1.41 \times 10^{-3} \text{ W}^{-1}$  quite well.

## 5. Conclusion

A cw intracavity frequency-doubled and frequency-stabilized ring Nd:YAP/KTP laser end-pumped by a fiber-coupled diode array has been achieved. The intensity fluctuation is better than  $\pm 1.5\%$ . The frequency stability is better than  $\pm 550$  kHz. An effective and simple method to enforce the intracavity frequency-doubled laser with a type II non-critical phase-matching crystal unidirectional operating and compensate the dispersion by means of a  $\lambda/4$  wave plate is presented.

## Acknowledgements

This work is supported by the National Nature Science Foundation (No. 19974021) and Nature

Science Foundation of Shanxi Province (No. 981030).

## References

- [1] V.M. Garmash, G.A. Ermakov, N.I. Paavlova, et al., *Sov. Tech. Phys. Lett.* 12 (1986) 505.
- [2] K.C. Peng, Q. Pan, H. Wang, et al., *Appl. Phys. B* 66 (6) (1998) 775.
- [3] Y. Zhang, H. Wang, X.Y. Li, K.C. Peng, et al., *Phys. Rev. A* 62 (2000) 023813.
- [4] Z.Y. Ou, S.F. Pereira, H.J. Kimble, *Appl. Phys. B* 55 (1995) 265.
- [5] S.F. Pereira, Z.Y. Ou, H.J. Kimble, *Phys. Rev. A* 62 (2000) 042311.
- [6] X.Y. Li, Q. Pan, J. Jing, K.C. Peng et al., *Quantum dense coding exploiting bright EPR beam*, arXiv: quant-ph/0107068 (to appear).
- [7] Q. Pan, T.C. Zhang, Y. Zhang, K.C. Peng, *Appl. Opt.* 37 (12) (1998) 2394.
- [8] Y.F. Chen, T.M. Huang, C.F. Kao, et al., *IEEE J. Quantum Electron.* 33 (8) (1997) 1424.
- [9] S.C. Tidwell, J.F. Seamans, M.S. Bowers, et al., *IEEE J. Quantum Electron.* 28 (4) (1992) 997.
- [10] T. Bear, *J. Opt. Soc. Am. B* 3 (9) (1986) 1175.
- [11] D.W. Anthon, D.L. Sipes, T.J. Pier, et al., *IEEE J. Quantum Electron.* 28 (4) (1992) 1148.
- [12] K.L. Martin, W.A. Clarkson, D.C. Hanna, *Opt. Lett.* 21 (1996) 875.
- [13] F. Hanson, P. Poirier, *J. Opt. Soc. Am. B* 12 (7) (1995) 1311;  
R. Wu, H. Shen, R. Zeng, et al., *Chin. J. Laser* 1 (5) (1992) 385;  
F. Hanson, *Opt. Lett.* 14 (13) (1989) 674.
- [14] J.K. Chee, B.S. Choi, *Opt. Commun.* 118 (1995) 289;  
F.C. Zumsteg, J.D. Bierlein, T.E. Gier, *J. Appl. Phys.* 47 (1976) 4980.
- [15] G.D. Boyd, D.A. Kleinman, *J. Appl. Phys.* 39 (1968) 3597.